Journal of the Serbian Chemical Society
JSCS-info@shd.org.rs • www.shd.org.rs/JSCS

ACCEPTED MANUSCRIPT

Journal of the Serbian Chemical Society
JSCS-info@shd.org.rs • www.shd.org.rs/JSCS
J. Serb. Chem. Soc. **00(0)** 1-15 (2026)
JSCS–13976
Original scientific paper
Published DD MM, 2026

Influence of fly ash fineness on cesium immobilization in geopolymers

GORDANA G. STANOJEVIĆ[1]*, MIROSLAV M. KOMLJENOVIĆ[1], JANA LJ. PETROVIĆ[2] AND RADA D. PETROVIĆ[3]

[1]*Institute for Multidisciplinary Research, National Institute of the Republic of Serbia, University of Belgrade, Kneza Višeslava 1, 11030 Belgrade, Serbia,* [2]*Innovation Center of the Faculty of Technology and Metallurgy, Ltd, 11060 Belgrade, Serbia, and* [3]*Faculty of Technology and Metallurgy, University of Belgrade, Karnegijeva 4, 11060, Belgrade, Serbia.*

(Received 16 May; revised 27 May; accepted 2 June 2026)

Abstract: The influence of fly ash (FA) fineness on cesium (Cs) immobilization in geopolymers was investigated by comparing samples synthesized in this study with those reported previously, as all samples were prepared at 95 °C with Cs contents of 2 and 5 wt.%. The effect of FA particle size distribution on physico-mechanical properties, gel structure development, and Cs leaching behavior was evaluated. Results show that FA fineness significantly affects the kinetics of geopolymerization and the development of mechanical properties. In general, Cs addition prolongs the setting time in G-FA, with longer setting times observed in G-FA based on coarser FA sample. These samples also showed lower compressive strengths, indicating that finer FA particles promote faster dissolution of aluminosilicate species and more rapid formation of the geopolymeric gel. Leaching behavior revealed that Cs release is diffusion-controlled regardless of FA fineness and Cs content, but the mean leachability index (L_{mean}) was lower in samples based on coarser FA particles, although in all cases it was higher than 9, which indicates effective Cs immobilization and satisfactory long-term stability of the material. Overall, FA fineness influences geopolymer reactivity, gel structure, and thus mechanical performance and effectiveness of Cs immobilization.

Keywords: alkaline activation; particle size distribution; radioactive waste; leaching; physico-mechanical properties.

INTRODUCTION

Geopolymers are formed as a product of alkaline activation of aluminosilicate materials, including fly ash (FA) from thermal power plants.[1] The main product of the reaction is a cross-linked, three-dimensional, predominantly amorphous aluminosilicate gel, consisting of SiO_4 and AlO_4 tetrahedra that are connected by oxygen. The negative charge resulting from the incorporation of the AlO_4 units

* Corresponding author. E-mail: gordana@imsi.bg.ac.rs
https://doi.org/10.2298/JSC260516030S

into the silicate structure is compensated by alkali metal cations from the activator solution,[2-4] mainly Na^+, which leads to the formation of N-A-S-H gel. Due to such a structure, these materials exhibit a high capacity for binding and stabilizing ionic species, which is why they have recently been intensively investigated for the immobilization of radionuclides.[10,11] Among the key radionuclides resulting from nuclear activities, ^{137}Cs is characterized by a moderate half-life (about 30 years),[7,8,12] high specific activity (3.2 TBq/g),[13] and high-energy decay,[14] which makes it highly dangerous and harmful to both the environment and human health.

Previous studies have investigated the influence of temperature and curing time, as well as Cs sources such as $CsNO_3$ and $CsOH{\cdot}H_2O$, on Cs immobilization in FA-based geopolymers.[15] It was observed that flexural strengths increased with increasing curing time, but they did not observe significant differences with curing temperature. However, in both cases (when Cs was added as $CsOH{\cdot}H_2O$ and as $CsNO_3$), the presence of Cs reduced flexural strengths. This effect was more significant when Cs was added as $CsNO_3$, probably due to the lower pH compared to $CsOH{\cdot}H_2O$. Moreover, these studies suggest that Cs is immobilized within the aluminosilicate gel matrix, which represents the main product of alkali activation. Li et al.[16] reported a similar immobilization mechanism and demonstrated that geopolymers exhibit higher Cs immobilization efficiency compared to Portland cement. Jang et al.[17] also evaluated Cs immobilization efficiency using different types of FA with varying chemical compositions, where the Al_2O_3 content ranged from approximately 22 to 27 wt.% and the CaO content from about 2.9 to 5.2 wt.%. Granulometric characteristics were not reported. Despite these compositional variations, the leachability index remained similar, reaching approximately 10 after 90 days of leaching. The influence of Cs on physico-chemical properties, such as setting time and mechanical strength, was not assessed. Jain et al.[18] demonstrated, using analysis of variance (ANOVA), that curing temperature has the most significant influence on Cs immobilization, contributing approximately 84.64 % to the overall effect, followed by the interaction between Cs content and temperature. The concentration of sodium hydroxide as an activator had only a minor influence (approximately 0.35 %). It was also found that at Cs concentrations higher than 8 %, pollucite ($CsAlSi_2O$) formation occurs, which likely resulted in a very high leachability index ranging from 11 to 14.[18,19]

Despite numerous studies, the utilization of geopolymers for the immobilization of radioactive waste, including Cs, remains largely unexploited in practice. This is mainly because the wide range of synthesis conditions makes it difficult to clearly identify the key factors governing FA reactivity and the resulting geopolymer's structure and properties. In addition to chemical and mineralogical composition,[2,21,22] which can differ significantly between sources and even within the same source, FA fineness is considered an important parameter

which influences FA reactivity. However, its role in Cs immobilization has not yet been investigated. In this study, FA from the thermal power plant "Nikola Tesla A", Obrenovac (Serbia), was used as the starting material for synthesizing Cs-containing geopolymers. During pneumatic transport at the thermal power plant, FA is separated into several fractions. In our previous study[22], the FA-4 fraction (finer particles) was used to synthesize Cs-containing geopolymers. In contrast, the present study uses the FA-3 fraction (coarser particles) to evaluate the influence of granulometric composition on Cs immobilization efficiency and physico-mechanical properties.

EXPERIMENTAL

Materials

The chemical composition of **FA-3** was determined using the **classical alkali melting method**, while the particle size distribution was determined by wet sieving. The obtained results are presented in Table I. According to the international ASTM C618 classification,[23] FA-3 belongs to Class F. Compared to FA-4,[22] FA-3 has a slightly higher SiO_2 content and a slightly lower Al_2O_3 content. The proportion of fine particles (< 45 μm) in FA-3 is lower than in FA-4 (92.5 %).

TABLE I. Chemical composition and particle size distribution of FA-3, wt. %.

Component	FA-3
Chemical composition	
SiO_2	58.2
Al_2O_3	20.2
Fe_2O_3	5.3
MnO	0.03
CaO	7.6
MgO	2.0
SO_3	2.2
Na_2O	0.5
K_2O	1.5
Loss on ignition at 1000 °C	1.6
Particle size	
< 45 μm	82.5
45-63 μm	6.8
63-100 μm	6.7
>100 μm	4.0

The geopolymers without and with Cs were prepared under the same conditions as in our previous study.[22] A sodium silicate solution with a modulus (oxide mass ratio n = SiO_2/Na_2O) of 1.5 was used as the activator. The solution was prepared by mixing a commercial sodium silicate solution (13.60 % Na_2O, 26.25 % SiO_2, 60.15 % H_2O; "Galenika-Magmasil", Serbia), with an initial modulus of 1.93, and sodium hydroxide (NaOH) (98.5 %, "Lach-Ner", Czech Republic).

Cesium chloride (99.9 % CsCl, Superlab, Serbia) was used as a source of the non-radioactive isotope $^{133}Cs^+$. Concentrated nitric acid (65 % HNO_3, Analar Normapur, EC) was

used to adjust the pH of the solutions obtained by the leaching and filtration procedure, and was intended for the determination of the concentrations of Cs, Si, and Al.

Synthesis of geopolymers pastes and mortars

The geopolymer pastes without and with Cs were prepared by mixing FA-3, alkaline activator, and water or CsCl solution. The geopolymer mortars were prepared by mixing FA-3, alkaline activator, water or CsCl solution, and standard sand, following the procedure of EN 196-1[24] as closely as possible. Depending on the Cs content (0 %, 2 % and 5 %), the samples were designated as G-FA-3-0Cs, G-FA-3-2Cs and G-FA-3-5Cs, respectively. The procedures for pastes and mortars preparation were the same as in the previous research[22] and are given in the Supplementary material.

Physico-mechanical properties

The setting time was monitored on geopolymer paste samples by using Vicat penetrating needle, according to EN 196-3 standard procedure.[25]

Compressive strengths of geopolymer mortars were determined according to EN 196-1[24] standard, using a Matest device.

Characterization of geopolymers

Mineralogical characterization was performed by XRD analysis using an X-ray diffractometer (Proto AXRD Benchtop) with CuKα X-rays, with 0.015° 2$\boldsymbol{\theta}$ steps, in the 5–80° 2$\boldsymbol{\theta}$ range. Crystal phases were identified using the "Crystallographica Search Match" software and the JCPDS-ICDD powder diffraction database.

Fourier transform infrared spectroscopy (FTIR) measurements were performed using a Perkin Elmer Spectrum Two spectrometer in attenuated total reflection (ATR) mode using a diamond crystal, in the range of 400–4000 cm^{-1}, with a resolution of 4 cm^{-1} and 4 replicates per sample.

Microstructural characterization was carried out using field emission scanning electron microscopy (FESEM) on a TESCAN Mira3 XMU electron microscope. Energy dispersive spectroscopy (EDS) analysis was performed on an INCAx-act LN2-free analytical silicon drift characteristic X-ray detector with PentaFET® Precision and Aztec 4.3 software package (Oxford Instruments) interfaced with a TESCAN Mira3 XMU. EDS analysis was conducted at 17 points per sample. Unreacted FA particles were excluded from the analyzed areas.

Leaching process

Leaching tests for the G-FA-3 samples were conducted according to the semi-dynamic leaching test ANSI/ANS-16.1-2003,[26] the details of which are presented in the Supplementary material. Based on the Cs leaching results, the leaching rates (LR), diffusion coefficient (D) and mean leachability index (L_{mean}) were calculated according to the equation S1, S3 and S5 which are presented in the Supplementary material.

RESULTS AND DISCUSSION

Physico-mechanical properties

Fig. 1 shows the setting time of G-FA-3 pastes at different Cs contents. All tested pastes met the requirement defined by EN 197-1 [27] standard, which states that the start of setting should not be earlier than 60 min. As can be seen, increasing the Cs content, prolonged both the initial and final setting times compared to the sample G-FA-3-0Cs. According to the relevant EN 197-1 standard,[27] the final

setting time must not exceed 600 min; however, both samples exceeded this limit. The deviation was more pronounced for the sample G-FA-3-5Cs, which showed the greatest delay in setting.

Also, in a previous study using a finer fraction of FA,[22] longer setting times were observed in samples containing Cs, which was mainly attributed to the slowing of condensation reactions. In the present study, the setting times were approximately twice as long as in the previous study. This can be attributed to a lower proportion of particles smaller than 45 μm in the FA used here, since the setting behavior depends on the dissolution rate of the starting material. This process is likely governed by the granulometric composition of FA, which influences the specific surface area of the particles and, consequently, the reactivity of the FA. Finer FA particles, due to their higher specific surface area, promote faster release of Si and Al species,[2,28] leading to accelerated gel formation and shorter setting times.

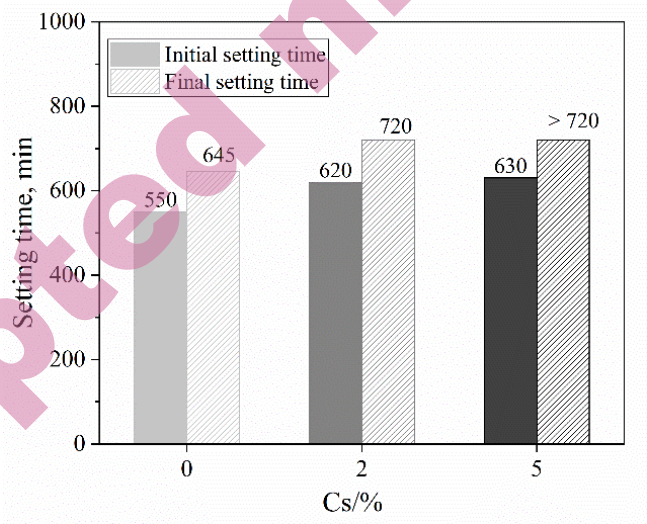

Fig. 1. Setting times of G-FA-3 samples

The compressive strengths of G-FA-3 mortars at different Cs contents are shown in Table II. All G-FA-3 samples, regardless of Cs content, exhibited compressive strength far above the minimum requirement of 3.4 MPa specified by NRC regulations for the immobilization of radioactive waste.[29] Increasing the Cs content to 5 % leads to a slight increase in compressive strength, in contrast to previous research,[22] which reported no significant change in mechanical properties with the addition of cesium. This behavior may be attributed to enhanced dissolution of FA and partial structural reorganization of the aluminosilicate gel in the presence of a larger amount of Cs. This is evident in samples based on FA-3,

which has lower intrinsic reactivity, where Cs likely promotes additional dissolution and contributes to a higher degree of gel formation. In the case of the finer system,[22] gel phase formation is predominantly governed by the matrix itself, limiting any additional influence of Cs, although a prolonged setting time was observed, as in this study.

Overall, the G-FA-3 samples exhibited lower compressive strength values compared to G-FA-4 (Table II), which can be attributed to differences in granulometric composition. Obviously, finer particles enable faster formation of aluminosilicate gel and thus better mechanical properties. These results indicate that granulometry plays a key role in governing the mechanical performance of geopolymer.

TABLE II. Compressive and flexural strengths G-FA-3 samples

Sample	G-FA-3-0Cs	G-FA-3-2Cs	G-FA-3-5Cs	G-FA-4-0Cs[22]
Compressive strengths, MPa				
	40.4±1.00	40.8±0.44	44.4±0.53	58.9±1.59
Relative compressive strength, MPa (relative to the sample G-FA-3-0Cs)				
	1.00	1.00	1.11	1.45
Relative compressive strength, MPa (relative to the sample G-FA-4-0Cs*)				
	0.68	0.69	0.75	1.00

XRD

The XRD patterns of FA-3 and G-FA-3 samples with varying Cs contents are presented in Fig. S-1 in Supplementary material. The XRD pattern of FA-3 shows crystalline phases characteristic for FA, as in the case of FA-4: quartz (SiO_2; JCPDS #89-8934), mullite ($Al_{5.33}Si_{0.67}O_{9.33}$; JCPDS #85-1460), hematite (Fe_2O_3; JCPDS #88-2359), anhydride ($CaSO_4$; JCPDS #72-0916) and feldspar ($NaAlSi_3O_8$; JCPDS #89-6423). In addition to these crystalline phases, calcite ($CaCO_3$; JCPDS #72-1937) is observed in G-FA-3 samples due to carbonation, which was also observed in previous research.[12,22] A reflection at 31.7º 2θ in the patterns of the Cs-containing samples, which increases with increasing Cs content, probably indicate a newly formed crystalline phases with Cs, similar as in the previous research.[12,22] These results show that granulometric composition does not affect the phase composition of FA and FA-based geopolymers.

FTIR

In Fig.2, the FTIR spectra of FA-3 and G-FA-3 samples, which are very similar to those of FA-4 and G-FA-4, are shown. The most intense band in the FTIR spectrum of FA-3 is located at 1058 cm^{-1} and originates from the asymmetric stretching vibrations of T-O-Si (T = Al, Si).[30] The bands of the symmetric stretching vibrations of Si-O-Si and Si-O-Al are observed at about 796, 780, 676,

611 cm^{-1}, while the bands of the symmetric bending vibrations of Si-O-Si and Si-O-Al are located at about 594, 555, and 450 cm^{-1},[30] very similar as for FA-4. The doublet at 796 and 780 cm^{-1} is mainly attributed to quartz, which remains inert during geopolymerization.[31] In the FTIR spectrum of the G-FA-3-0Cs sample, the most intense band become sharper and more intense, and are shifted towards a lower wavenumber, from 1058 cm^{-1} in FA-3 to 1005 cm^{-1} in the G-FA-3-0Cs sample (Fig. 2a). The shift of the most intense band indicates a decrease in the T-O-T angle and elongation of the T-O-Si bonds, and is most often associated with the incorporation of Al into the gel structure during the formation of an aluminosilicate gel.[30,32-35] Such shift was also observed in the case of FA-4-based geopolymer. The bands at 676 and 594 cm^{-1} in the G-FA-3-0Cs sample cannot be observed, probably due to the dissolution of FA-3 during geopolymerization, while the band at 555 cm^{-1} remains unchanged during geopolymerization (Fig. 2b). This band probably belongs to mullite.[36] A similar observation was made when using FA-4.[22] The bands at 1443 and 875 cm^{-1} are attributed to the stretching vibrations of the C-O bond in the carbonate group, indicating the presence of carbonate,[15,30] which is also consistent with the XRD analysis. The broad band at about 3390 cm^{-1} and the band at 1641 cm^{-1} originate from the bending and stretching vibrations of the O-H and H-O-H water molecules, which are physically and chemically bound in the N-A-S-H gel structure.[15,30]

In the FTIR spectra of G-FA-3 samples with the addition of Cs, a slight shift of the most intense band was observed from 1005 cm^{-1} (for the G-FA-3-0Cs sample) to 1003 cm^{-1} and 999 cm^{-1} for the G-FA-3-2Cs and G-FA-3-5Cs samples, respectively (Fig. 2a). This slight shift of the most intense band with an increase in the Cs content in the G-FA-3 samples could indicate some kind of structural reorganization of the N-A-S-H gel, *i.e.*, an increase in the proportion of Si-O-Al bonds and a higher degree of crosslinking within the gel network. This structural reorganization leads to the formation of a more compact and stable matrix, which is in an agreement with the observed increase in strength, especially at higher Cs contents (5 %). The shift to lower wavenumbers was not observed in samples prepared with FA-4, which can be attributed to the higher proportion of finer particles (particles smaller than 45 μm), resulting in a less pronounced effect of Cs addition, which could not be detected by FTIR analysis.

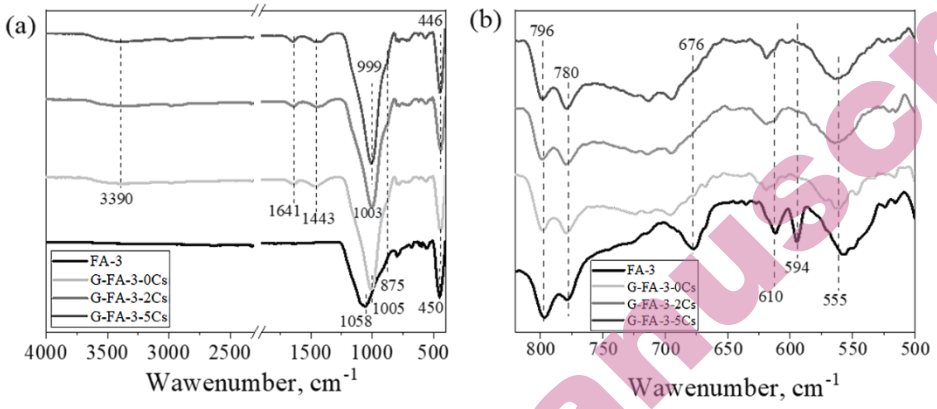

Fig 2. FTIR spectra of FA-3 and G-FA-3 samples (a) full spectral range and (b) expanded view in the 820–500 cm^{-1} range

FESEM/EDS

As shown in Fig. S-2 in Supplementary material, the addition of Cs did not significantly affect the microstructure of G-FA-3 samples, as was the case with FA-4-based samples.

Fig. 3 presents the distribution of atomic ratios for the main elements present in the aluminosilicate gel. Overall, the high variability in the measured atomic ratios, as in the case of FA-4-based samples, indicates the heterogeneous nature of the aluminosilicate gel. Notwithstanding, the findings reveal a decrease in the Si/Al ratio with the incorporation of Cs, consistent with previous research,[22] which indicates the increase in Al content in the gel. This aligns with the FTIR analysis, where a shift of the most intense band toward lower wavenumbers was observed (Fig. 2a). The decrease in the Na/Al ratio with the addition of Cs suggests partial substitution of charge-balancing Na^+ ions by Cs^+ ions in the aluminosilicate gel structure. Similar trends were observed in the G-FA-4 samples. However, due to the potential migration of Na^+ ions under the electron beam during EDS analysis, the Na/Al ratio should be interpreted as a relative trend rather than an absolute value.[37] This may also explain the Na/Al ratio lower than 1 in the G-FA-3-0Cs sample.

It is evident that Si/Al ratios are lower for G-FA-3 than for G-FA-4 samples, indicating a higher proportion of Al in the G-FA-3 gel. It is known that, in the initial phase of the reaction, a gel with higher aluminium content is formed, due to the greater solubility of aluminium from the amorphous phase of FA in comparison to silicon. As the reaction progresses, a gel with a higher proportion of silicon is formed. Consequently, it can be hypothesized that the alkaline activation reaction is slower in FA-3 due to its coarser particles, resulting in less developed gel formation. Due to lower degree of geopolymerization, G-FA-3 samples exhibited

lower compressive strength in comparison with the G-FA-4 samples, as discussed in the preceding paragraph.

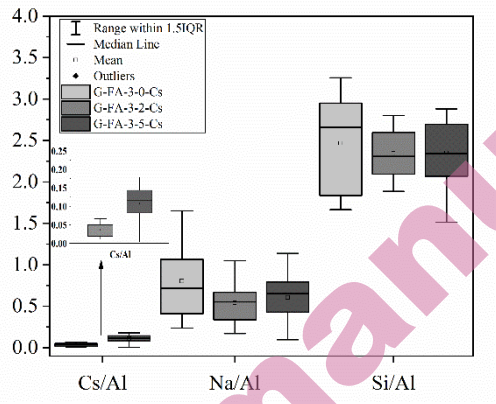

Fig.3. Distribution of the atomic ratios of main elements in G-FA-3 samples with varying Cs contents Inset shows Cs/Al ratio due ti its lower magnitude.

Leaching process

Leaching of Cs

The leaching kinetics of Cs from G-FA-3 samples were investigated based on the cumulative leached concentration and the leaching rate, calculated according to equation S1 in Supplementary material, as a function of leaching time. The obtained cumulative concentrations and corresponding leaching rates are presented in Fig. 4.

The leaching rate of Cs was highest during the first 2 h (Fig. 4b), similar to the case of G-FA-4 samples.[22] This trend is characteristic of diffusion-controlled leaching, where, after the initial leaching of surface-available ions, the transport of Cs^+ ions occurs by diffusion through the increasingly compact geopolymer matrix. In general, Cs leaching rates were higher when the Cs content in the sample was 5 %, indicating that the degree of Cs immobilization decreases with increasing Cs content, probably due to a higher proportion of weakly bound Cs^+ ions. These ions are most likely located on the surface or in the pore solution of the aluminosilicate gel, which enables their faster leaching. This effect is also clearly reflected in the cumulative Cs leaching values in samples with higher Cs content. After five days of leaching, the cumulative leached Cs concentration was approximately 3.8 times higher in the sample with 5 % Cs compared to the sample with 2 % Cs, although the Cs content in sample G-FA-3-5Cs is 2.5 times greater than in sample G-FA-3-2Cs. In comparison to G-FA-4 samples (Fig. S3), cumulative concentrations of leached Cs were higher, regardless of the comparable initial leaching rates.[22] It can be seen that LR values in later periods are higher for G-FA-3 samples, which

indicates their less compact matrix and easier Cs leaching, meaning lower immobilization efficiency.

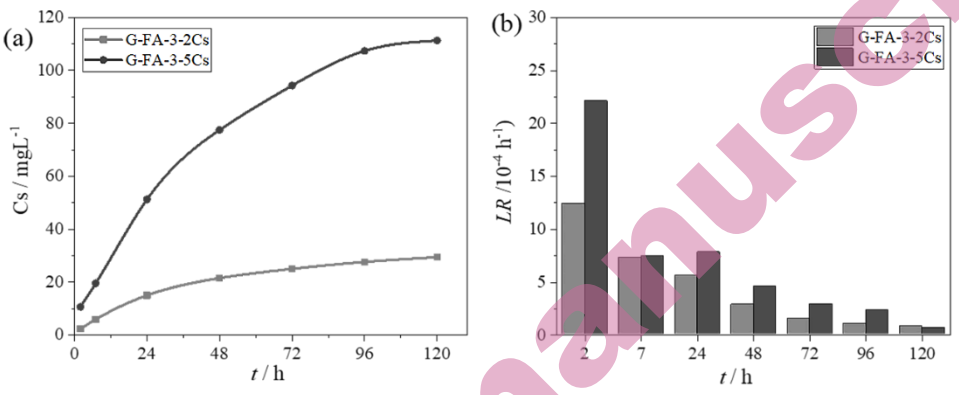

Fig 4. a) The cumulative concentration of leached Cs and b) the leaching rate of Cs. (Analytical uncertainty in each point is approximately 1 %)

Leaching of Si and Al

The cumulative leached concentrations of Si and Al are presented in Fig. 5. The very low concentration of leached Al indicates the stability of the formed gel in deionized water, regardless of the high concentration of leached Si. As hypothesized in previous research,[22] the leached Si originated mainly from unreacted sodium silicate used as the alkaline activator. This assumption is further supported by the consistently high pH values (11 – 11.5) of the leaching solution throughout the entire leaching period, which indicates the leaching of unreacted alkaline activation solution. Higher concentrations of leached Si in the case of G-FA-3 (Fig. 5a and S-4a) are probably the result of a slower alkaline activation reaction, resulting in larger amounts of residual, unreacted sodium silicate in the gel pores compared to G-FA-4.[22] It was also observed that the addition of Cs leads to a decrease in the leaching of Si and Al, particularly at a Cs content of 5 %, indicating an acceleration of alkaline activation and the formation of a more stable gel structure, consistent with the observed increase in compressive strength.

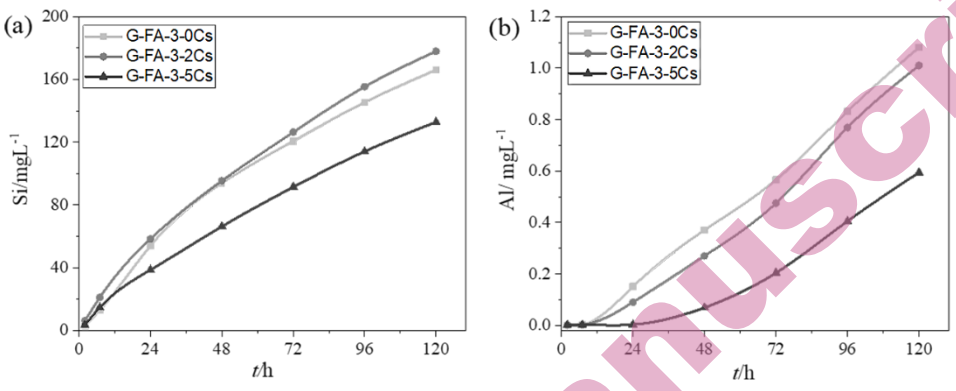

Fig. 5. Cumulative leaching behavior of the main aluminosilicate gel components: (a) Si, (b) Al. (Analytical uncertainty in each point is approximately 1 %)

Mechanism of Cs leaching and effectiveness of Cs immobilization

The diffusion model proposed by de Groot and van der Sloot was used to determine the primary mechanism of Cs leaching, based on the slope of the relationship between the logarithm of the cumulative leached Cs (B_t) and the logarithm of time (t).[38,39] The value of B_t can be obtained from equation 1:

$$B_t = \frac{c_t * V_t}{S} \quad (1)$$

where B_t is the cumulative concentration of leached Cs over time t, mgm^{-2}); t is the contact time, s; C_t is the concentration of leached Cs over time t, mgL^{-1}; V_t is the volume of the leaching medium, L; S is the geometric surface area of the sample, m^2. A slope value between 0.4 and 0.6 indicates diffusion-controlled leaching. When the slope value is greater than 0.6, the primary leaching mechanism is dissolution (it implies that dissolution on the surface is faster than the diffusion of ions from the interior of the sample), while for a slope value less than 0.4, surface leaching is the primary mechanism. The obtained values are shown in Fig. 6.

As can be seen from Fig. 6, the primary mechanism of Cs leaching is diffusion, regardless of the Cs content. Similar Cs leaching behavior was observed for G-FA-4 samples, but the slopes were slightly lower (Fig. S2 in Supplementary material).[22] This indicates that the difference in the granulometry of the FA has no significant effect on the mechanism of Cs leaching from the geopolymer, as observed for the physico-mechanical characteristics.

The mean leachability index (L_{mean}) of Cs from G-FA-3-2Cs and G-FA-3-5Cs was calculated according to equation S5 in Supplementary material. L_{mean} was 9.4 and 9.1 for samples with 2 % and 5 % Cs, respectively. The obtained L_{mean} are higher than 6, which is the minimum value for a material to be considered suitable for Cs immobilization, according to the NRC criterion.[29]

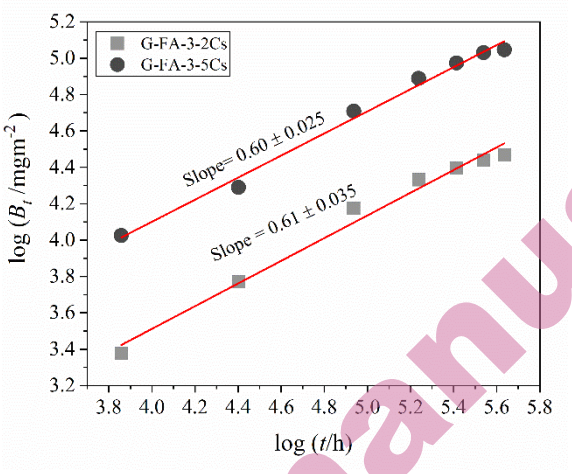

Fig. 6. The leaching mechanism of Cs from G-FA-3

The corresponding values for G-FA-4-2Cs and G-FA-4-2Cs were 9.7 and 9.3 for 5 days of leaching. Based on presented results, the slightly lower L_{mean} for G-FA-3 can be attributed to the formation of a less compact and more permeable gel structure due to lower reactivity of the coarser FA particles.

CONCLUSION

In this study, the influence of fly ash (FA) particle size distribution on Cs immobilization was investigated. Geopolymers were synthesized using fly ash (FA-3) with approximately 82 wt. % of particles smaller than 45 μm, at 95 °C for 24 h, and Cs contents of 2 and 5 wt.%. The obtained results were compared with literature data for geopolymers prepared under identical experimental conditions using finer FA-4, with approximately 92 wt. % of particles smaller than 45 μm.

The FA-3-based geopolymers (G-FA-3) showed that the addition of Cs prolonged the initial and final setting times, indicating a slowdown of condensation reactions, similar to that observed in G-FA-4 samples. However, longer setting times were recorded for G-FA-3 compared to FA-4-based geopolymers (G-FA-4). The addition of Cs also increased compressive strength at 5 wt.% Cs in the G-FA-3 samples, but compared to G-FA-4, the compressive strengths were lower, which is attributed to the slower reaction of coarser FA-3 particles. The slower reaction kinetics likely led to the formation of a less compact aluminosilicate gel structure, which is reflected in the generally lower compressive strength values of G-FA-3 compared to G-FA-4.

The leaching behavior confirmed that Cs release was diffusion-controlled in all systems, independent of FA granulometry, with mean leachability index (L_{mean}) values of 9.7 and 9.3 for G-FA-3 at 2 and 5 wt.% Cs, respectively. Nevertheless, the slightly higher Cs release observed for G-FA-3 compared to G-FA-4 is

consistent with the formation of a less compact gel network resulting from the lower reactivity of the coarser FA particles.

Overall, the results confirm that both FA fractions with different particle size distributions can be successfully applied for Cs immobilization. Although the influence of Cs on setting behavior, mechanical performance, and leaching resistance follows the same general trends as those observed for G-FA-4, these effects are more pronounced in G-FA-3 due to the lower reactivity of the coarser FA fraction. These findings highlight the importance of optimizing FA granulometry to improve matrix compactness and mechanical performance without compromising long-term environmental stability.

Acknowledgements: This research was financially supported by the NATO SPS programme (project G5402) and the Ministry of Science, Technological Development and Innovation of the Republic of Serbia through project contracts No. 451-03-33/2026-03/200053, 451-03-34/2026-03/200135 and 451-03-33/2026-03/200287. The authors would like to thank Dr. Ljiljana Kostić-Kravljanac (Institute for Multidisciplinary Research, National Institute of the Republic of Serbia, Belgrade, Serbia) for assistance in acquiring the ICP-OES data.

И З В О Д

ИСПИТИВАЊЕ УТИЦАЈА ГРАНУЛОМЕТРИЈСКОГ САСТАВА ЕЛЕКТРОФИЛТЕРСКОГ ПЕПЕЛА НА ИМОБИЛИЗАЦИЈУ ЦЕЗИЈУМА ГЕОПОЛИМЕРИМА

ГОРДАНА Г. СТАНОЈЕВИЋ[1]*, МИРОСЛАВ М. КОМЉЕНОВИЋ[1], ЈАНА Љ. ПЕТРОВИЋ[2], РАДА Д. ПЕТРОВИЋ[3]

[1]Институт за мултидисциплинарна истраживања, Институт од националног значаја за Републику Србију, Универзитет у Београду, Кнеза Вишеслава 1, 11030 Београд, Србија, [2]Иновациони центар Технолошко-металуршког факултета, 11060 Београд, Србија, и [3]Технолошко-металуршки факултет, Универзитет у Београду, Карнегијева 4, 11060, Београд, Србија.

Утицај гранулометријског састава електрофилтерског пепела (ЕФП) на имобилизацију цезијума геополимерима испитан је поређењем узорака синтетисаних у овом раду, са резултатима датим у претходним истраживања. Сви узорцои су припремани на 95 °C при уделу Cs од 2 и 5 mas.%. Испитан је утицај расподеле величине честица ЕФП на физичко-механичка својства, структуру гела и излуживање Cs. Резултати показују да гранулометријски састав значајно утиче на кинетику геополимеризације и развој механичких својстава. Генерално, додавање Cs продужава време везивања Г-ЕФП, при чему су дужа времена везивања уочена код Г-ЕФП са крупнијим честицама ЕФП. Такође, Г-ЕФП добијени коришћењем ЕФП са крупнијим честицама су показали ниже чврстоће при притиску, што указује да финије честице ЕФП подстичу брже растварање алуминосиликатних врста и брже формирање геополимерног гела. Излуживање Cs је дифузионо контролисано без обзира на величину честица ЕФП и удео Cs, иако је средњи индекс излуживања (L_{sr}) био нешто нижи у узорцима са крупнијим честицама ЕФП (L_{sr} за све узорке био је већи од 9). Генерално, гранулометријска својства ЕФП утичу на реактивност геополимера, структуру гела, а самим тим и на механичка својства и ефикасност имобилизације Cs.

(Примљено 16. маја; ревидирано 27. маја; прихваћено 2. јуна 2026.)

REFERENCES

1. J. Davidovits, *Geopolymer chemistry and applications*, 5th ed., Geopolymer Institute, Saint-Quentin, France, 2020, p. 311 (ISBN: 9782954453118)
2. P. Duxon, A. Fernández-Jiménez, J. L. Provis, G. C. Lukey, A. Palomo, J. S. J. van Deventer, *J. Mater. Sci.* **42** (2007) 2917 (https://doi.org/10.1007/s10853-006-0637-z)
3. J. L. Provis, J. S. J. van Deventer, *Geopolymers: Structure, Processing, Properties and Industrial Applications,* Woodhead Publishing, Cambridge, UK, 2009, p. 89 (https://doi.org/10.1533/9781845696382)
4. J. L. Provis, J. S. J. van Deventer, *Alkali-Activated Materials: State-of-the-Art Report*, RILEM TC 224-AAM. Springer/RILEM, Dordrecht, 2014, p. 98 (https://doi.org/10.1007/978-94-007-7672-2)
5. C. Shi, A. Fernández-Jiménez, *J. Hazard. Mater.* **B137** (2006) 1656 (https://doi.org/10.1016/j.jhazmat.2006.05.008)
6. R. O. Abdel Rahman, R. Z. Rakhimov, N. R. Rakhimova, M. I. Ojvan, *Cementitious Materials for Nuclear Waste Immobilization*, John Wiley & Sons Ltd., Chichester, United Kingdom, 2015, p. 8 (https://doi.org/10.1002/9781118511992)
7. Y. Zhu, Z. Zheng, Y. Deng, C. Shi, Z. Zhang, *Cem. Concr. Compos*. **126** (2022) 104377 (https://doi.org/10.1016/j.cemconcomp.2021.104377)
8. J. Liu, Y. Xu, J. Wang, W. Zhang, J. Ye, R. Wang, *J. Aust. Ceram. Soc*. **60** (2024) 1131 (https://doi.org/10.1007/s41779-024-01018-6)
9. S. Jain, O. Onuaguluchi, N. Banthia, T. Troczynski, *J. Am. Ceram. Soc*. **108** (2024) e20131 (https://doi.org/10.1111/jace.20131)
10. E. Mukiza, Q. T. Phung, S. C. Seetharam, T. N. Nguyen, C. Bruggeman, G. De Schutter, *J. Environ. Manag.* **370** (2024) 122746 (https://doi.org/10.1016/j.jenvman.2024.122746)
11. M. Houhou, N. Leklou, H. Ranaivomanana, J. D. Penot, S. de Barros, *Discov. Appl. Sci*. **7** (2025) 126 (https://doi.org/10.1007/s42452-025-06536-x)
12. M. Komljenović, G. Tanasijević, N. Džunuzović, J. L. Provis, *J. Hazard. Mater.* **388** (2020) 121765 (https://doi.org/10.1016/j.jhazmat.2019.121765)
13. S. Jain, N. Banthia, T. Troczznski, *Cem. Concr. Compos.* **133** (2022) 104679 (https://doi.org/10.1016/j.cemconcomp.2022.104679)
14. M. I. Ojovan, W. Lee, S. Kalmykov, *Short-lived waste radionuclides, in: An introduction to nuclear waste immobilization*, Elsevier, Oxford, United Kingdom, 2019, p. 8 (https://doi.org/10.1016/C2017-0-03752-7)
15. A. Fernández-Jiménez, D. E. Macphee, E. E. Lachowski, A. Palomo, *J. Nucl. Mater.* **346** (2005) 185 (https://doi.org/10.1016/j.jnucmat.2005.06.006)
16. Q. Li, SZ. Sun, D. Tao, Y. Xu, P. Li, H. Cui, J. Zhai, *J. Hazard. Mater.* **262** (2013) 325 (https://doi.org/10.1016/j.jhazmat.2013.08.049)
17. J. G. Jang, S. M. Park, H. K. Lee, *J. Hazard. Mater.* **318** (2016) 339 (https://doi.org/10.1016/j.jhazmat.2016.07.003)
18. S. Jain, N. Banthia, T. Troczynski, *J. Clean. Prod.* **380** (2022) 134984 https://doi.org/10.1016/j.jclepro.2022.134984)
19. S. Jain, N. Banthia, T. Troczynski, *Cem. Concr. Compos.* **133** (2022) 104679 (https://doi.org/10.1016/j.cemconcomp.2022.104679)
20. M. Komljenovic, Z. Bascarevic, V. Bradic, *J. Hazard. Mater.* **181** (2010) 35 (https://doi.org/10.1016/j.jhazmat.2010.04.064)

21. V. Nikolić, M. Komljenović, Z. Baščarević, N. Marjanović, Z. Miladinović, R. Petrović, *Constr. Build. Mater.* **94** (2015) 361 (https://doi.org/10.1016/j.conbuildmat.2015.07.014)
22. G. G. Stanojević, M. M. Komljenović, N. M. Džunuzović, S. S. Lazarević, J. L. Provis, R. D. Petrović, *Constr. Build. Mater.* **500** (2025) 144217 (https://doi.org/10.1016/j.conbuildmat.2025.144217)
23. ASTM C618-25a: *Standard Specification for Coal Fly Ash and Raw or Calcined Natural Pozzolan for Use in Concrete* (2025)
24. EN 196-1:2008: *Methods of testing cement - part 1: determination of strength* (2008)
25. EN 196-3:2010: *Methods of testing cement Part 3: Determination of setting times and soundness* (2010)
26. ANSI/ANS-16.1-2003 (R2017): *Measurement of the leachability of solidified low-level radioactive wastes by a short-term test procedure* (2003)
27. EN 197–1:2011: *Cement - Part 1: Composition, specifications and conformity criteria for common cements* (2011)
28. R. Gao, Z. Zhou, J. Yang, J. Zhang, *Open Ceram.* **20** (2024) 100680 (https://doi.org/10.1016/j.oceram.2024.100680)
29. NRC, Wasteform Technical Position, Revision 1, 1991.
30. P. Rozek, M. Król, W. Mozgawa, *Spectrochim. Acta A* **198** (2018) 283 (https://doi.org/10.1016/j.saa.2018.03.034)
31. W. K. W. Lee, J. S. J. van Deventer, *Langmuir* **19** (2003) 8726 (https://doi.org/10.1021/la026127e)
32. G. Kovalchuk, A. Fernández-Jiménez, A. Palomo, *Fuel* **86** (2007) 315 (https://doi.org/10.1016/j.fuel.2006.07.010)
33. C. A. Rees, J. L. Provis, G. C. Lukey, J. S. J. van Deventer, *Langmuir* **23** (2007) 8170 (https://doi.org/10.1021/la700713g)
34. A. Hajimohammadi, J. L. Provis, J. S. J. van Deventer, *Chem. Mater.* **22** (2010) 5199 (https://doi.org/10.1021/cm101151n)
35. S. L. A. Valcke, P. Pipilikaki, H. R. Fischer, M. H. W. Verkuijlen, E. R. H. van Eck, *Mater. Struct.* **48** (2014) 557 (https://doi.org/10.1617/s11527-014-0432-2)
36. M. Criado, A. Fernández-Jiménez, A. Palomo, *Micropor. Mesopor. Mater.* **106** (2007) 180 (https://doi.org/10.1016/j.micromeso.2007.02.055)
37. M. Rowles, B. O'Connor, *J. Mater. Chem* **13** (2003) 1161 (https://doi.org/10.1039/b212629j)
38. G.J. de Groot, H. A. van der Sloot, *Determination of Leaching Characteristics of Waste Materials Leading to Environmental Product Certification, in* ASTM *Selected Technical Papers STP1123, Stabilization and Solidification of Hazardous, Radioactive, and Mixed Wastes: 2nd Volume*, T.C. Gilliam, C.C. Wiles, Eds., ASTM, West Conshohocken, United States, 1992, p. 149 (https://doi.org/10.1520/stp19548s)
39. H.A. van der Sloot, J.J. Dijkstra, *Development of Horizontally Standardized Leaching Tests for Construction Materials: a Material Based or Release Based Approach?*, Energy Research Centre of the Netherlands, 2004 (https://doi.org/10.13140/RG.2.2.11986.76486).